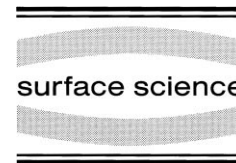




ELSEVIER

Surface Science 418 (1998) 22–31



Evolution of surface morphology of vicinal Si(111) surfaces after aluminum deposition

C. Schwennicke, X.-S. Wang¹, T.L. Einstein, E.D. Williams*

Department of Physics, University of Maryland, College Park, MD 20742-4111, USA

Received 9 March 1998; accepted for publication 13 August 1998

Abstract

We have studied changes in surface morphology of vicinal Si(111) surfaces with a miscut of 1.3° in the $[\bar{2}11]$ direction after Al deposition at elevated temperatures. The clean surface phase separates into a (111)-oriented phase and a stepped phase. Submonolayer Al deposition at 650°C , the normal preparation temperature of the Al/Si(111)- $(\sqrt{3} \times \sqrt{3})\text{R}30^\circ$ structure, only induces minor changes in the surface morphology. However, after Al deposition at temperatures above the order–disorder phase transition temperature, the step bunches break apart into a uniform array of single height steps with an average step–step separation determined by the macroscopic miscut. From a quantitative analysis of the amount of meandering of steps and the terrace width distribution, we determined the diffusivity of steps and the strength of the repulsive step–step interaction. The repulsive interaction between steps is enhanced by the Al adsorption compared to both the high-temperature (1×1) and (7×7) phases of the clean surface. © 1998 Elsevier Science B.V. All rights reserved.

Keywords: Aluminum; Epitaxy; LEED; Scanning Tunneling Microscopy; Silicon; Stepped single crystal surfaces; Surface morphology; Surface thermodynamics; Vicinal single crystal surfaces

1. Introduction

Since aluminum is the most widely used material for metallization in semiconductor technology, the study of the aluminum–silicon interface has technological importance. Most surface studies have concentrated on the atomic and electronic structure of the variety of reconstructions observed for this system [1–4]. None of these publications,

however, addresses the question of metal-induced changes in the surface morphology. This question is of particular interest for semiconductor technology, since fabricated nanostructures in the silicon substrate have to be stable during further processing, including metallization to create metal gates and interconnects.

The main subject of this paper is the evolution of the nanostructure of the vicinal Si(111) surface after aluminum deposition at elevated temperatures. Vicinal Si(111) surfaces with different orientations of the miscut angle have been studied in great detail using diffraction and microscopic techniques. In particular, the faceting of vicinal Si(111) surfaces that are misoriented in the $[\bar{2}11]$

* Corresponding author. Fax: +1 301 405 7993; e-mail: williams@surface.umd.edu

¹ Present address: Department of Physics, Hong Kong University of Science and Technology, Clear Water Bay, Kowloon, Hong Kong.

direction has been investigated, and a complete orientation and temperature-dependent phase diagram has been mapped out [5,6].

The substrates that we used for aluminum deposition were Si(111) samples with a miscut in the $[\bar{2}11]$ direction. Independent of the miscut angle, these surfaces are unstable against faceting below the (7×7) to (1×1) phase transition, which occurs at approximately 850°C on the clean, unstepped surface, and spontaneously form (111) oriented terraces with a width of about 900 Å separated by bunches of steps [7]. The height of the step bunches is of course determined by the macroscopic miscut angle.

We show in this paper that this surface morphology can be changed dramatically by aluminum adsorption at sufficiently high temperatures, where the mobility of atomic steps is large enough to achieve a new equilibrium structure. We also show that, assuming an equilibrated crystal surface, quantitative information about kink formation energies and step interactions can be obtained from a statistical analysis of STM images. In particular, the analysis of the terrace width distribution (TWD) of the aluminum-covered surface will allow us to determine adsorbate-induced changes in the step–step interaction [8].

Terrace width distributions of a variety of surfaces have been measured with microscopic techniques in recent years. Distributions characteristic of repulsive step–step interactions [9–12], attractive step–step interactions [13] and non-interacting steps [14] have been found for clean metal and semiconductor surfaces. For vicinal Ag(110) surfaces, there was even evidence for an oscillatory interaction as a function of the interstep distance [15]. However, it is reasonable to expect that adsorbate-induced modification of the step–step interaction can be profound. In this work, we investigate this effect directly by comparing the step distributions on clean and Al-covered Si(111).

2. Experimental

The experiments were performed in a standard UHV system with a base pressure below 4×10^{-11} Torr. The system was equipped with a

LEED system and a home-made scanning tunneling microscope. Si wafers (As-doped, $10 \text{ m}\Omega \cdot \text{cm}$) used in the experiments were misoriented by 1.3° towards the $[\bar{2}11]$ direction. The samples were rinsed in methanol and deionized water prior to loading into the vacuum chamber. The samples were cleaned in UHV by flashing them quickly to 1250°C for 1 min followed by a quench to 900°C. To obtain the equilibrium morphology on the clean surface, the samples were cooled down very slowly (0.2 K s^{-1}) through the (1×1) -to- (7×7) -phase transition [10].

Al was evaporated from an Al_2O_3 crucible that was heated by a tungsten filament wrapped around the crucible [16]. Since the Al/Si(111) phase diagram has been mapped out in great detail [4], the well-known phase boundaries between different reconstructions can be used to calibrate the aluminum coverage. In our experiments, we calibrated the Al deposition rate by measuring the phase boundaries between the (7×7) , the $(\sqrt{3} \times \sqrt{3})\text{R}30^\circ$ and the $(\sqrt{7} \times \sqrt{7})\text{R}19.1^\circ$ reconstructions at coverages of about 0.25 and 0.4 monolayers while keeping the substrate temperature at 600°C. Heating at temperatures above 700°C is complicated by the onset of Al diffusion into the bulk and, above 800°C, by substantial rates of Al desorption. Typical deposition rates used in the experiment were about 0.5 ML min^{-1} .

The samples were annealed by direct-current heating. Control experiments in which we monitored the sample morphology after heating with reversed direction of direct current showed no differences in the sample morphology. The sample temperature was measured with an infra-red pyrometer, which was calibrated against an optical pyrometer. The STM images shown in this paper have been acquired with a tip bias of -2.0 V and a tunneling current of 1.0 nA . All STM measurements were carried out at room temperature. The images are not corrected for thermal drift.

3. Results

An STM image of the clean Si(111) surface misoriented by 1.3° towards the $[\bar{2}11]$ direction is

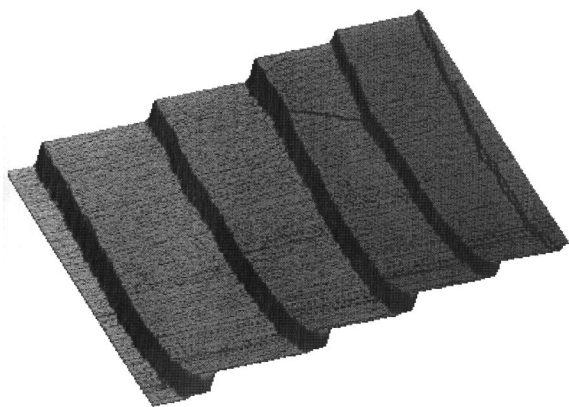


Fig. 1. $4000 \times 4000 \text{ \AA}^2$ STM image of a clean Si(111) surface with a miscut of 1.3° towards the $[\bar{2}11]$ direction. Terraces with an average width of about 900 \AA are separated by step bunches containing six to ten single-layer-height steps. Occasionally, crossing steps with a single-layer height are observed, as can be seen on one of the terraces. The $[\bar{2}11]$ direction is orthogonal to the average step edges and in the downhill direction.

shown in Fig. 1. After the preparation described above, including a very slow cooling through the (1×1) -to- (7×7) -phase transition, the surface was found to consist of terraces with a typical width of 900 \AA , separated by bunches of six to ten steps.

In agreement with other experiments reported in the literature [1,4], a $(\sqrt{3} \times \sqrt{3})R30^\circ$ reconstruction was seen with LEED after deposition of $1/3 \text{ ML}$ of aluminum at 650°C . The surface morphology that we observed following deposition at this temperature changed little compared to the clean surface. The width of the large terraces was still about 900 \AA , and steps were still concentrated in bunches. However, a closer examination of the step bunches revealed a slight spread. Individual terraces with $(\sqrt{3} \times \sqrt{3})R30^\circ$ reconstruction could be resolved in the step bunch after aluminum deposition. As discussed below, we believe that this is a metastable morphology.

In the following experiment, aluminum was deposited on the surface at 770°C . At this temperature, the Al desorption (or bulk segregation) rate is still sufficiently small, compared to the deposition rate, that a coverage of $1/3 \text{ ML}$ can be achieved without any significant increase in deposition time. At this temperature, however, Al is no longer ordered in a $(\sqrt{3} \times \sqrt{3})R30^\circ$ structure but



Fig. 2. $2800 \times 2800 \text{ \AA}^2$ STM image of a Si(111) surface with a miscut of 1.3° towards the $[\bar{2}11]$ direction after deposition of a third of a monolayer of aluminum at a temperature of 770°C . After deposition, the sample was quenched to room temperature. The image was taken at room temperature. The surface now consists of an array of single-layer-height steps. The initial positions of the step bunches are no longer visible. The $[\bar{2}11]$ direction is orthogonal to the average step edge direction and in the downhill direction.

is disordered on the surface: only (1×1) spots can be seen in the LEED pattern at this temperature. As investigated earlier, the phase transition between the ordered $(\sqrt{3} \times \sqrt{3})R30^\circ$ structure and the disordered (1×1) at about 765°C is approximately reversible [17].

Fig. 2 shows the morphology of the surface after deposition of $1/3 \text{ ML}$ of aluminum at 770°C . To avoid any changes in the surface Al coverage during cooling, the sample was quenched to room temperature immediately after deposition at a rate of more than 100 K s^{-1} . Obviously, the morphology of the surface has changed dramatically compared to the structure shown in Fig. 1. The surface now consists of an array of approximately equally spaced single-layer-height steps. The average spacing is $136 \pm 2 \text{ \AA}$, consistent with the macroscopic miscut of 1.3° and a step height of 3.14 \AA . The initial positions of the step bunches and the (111) facets can no longer be seen in the images. A sharp $(\sqrt{3} \times \sqrt{3})R30^\circ$ LEED pattern can be observed after the rapid quench, indicating that the adsorbate overlayer has had a sufficient length of time to form a long-range ordered superstructure during the quench. Since we lowered the

temperature rapidly from the deposition temperature, we must question whether the uniformly stepped morphology is the equilibrium structure corresponding to the $(\sqrt{3} \times \sqrt{3})R30^\circ$ overlayer. (The alternative possibility is that the uniformly spaced steps are characteristic only of the disordered overlayer, and some different morphology characteristic of the low-temperature phase did not have time to form during the quench.) Unfortunately, the obvious experiment of cooling slowly through the transition cannot be performed, because diffusion of Al into the bulk substantially reduces the Al surface coverage, changing the ordered overlayer sequentially to the structures characteristic of lower Al coverage. In continuing work on this system (Q. Gu, E.D. Williams, unpublished results, 1998), we have addressed this problem by deposition just below the transition temperature and by sequential anneals to temperatures both above and below the transition temperature. We find that the uniformly stepped phase is stable as long as the $(\sqrt{3} \times \sqrt{3})$ overlayer is fully formed. If the Al coverage is decreased by diffusion into the bulk, (111) terraces nucleate on the stepped surface, and the steps begin to form into bunches. The number of nuclei and the angle of the bunches increase with decreasing Al coverage. As a result of these observations, we conclude that the uniformly stepped surface is the equilibrium morphology when the $(\sqrt{3} \times \sqrt{3})R30^\circ$ overlayer is present.

The rapid quench through the transition raises the question of the appropriate temperature to be used in analyzing the experimental data. In Fig. 3, an STM image of the local atomic structure of a single-layer-height step is shown. For the tunneling conditions used in Fig. 3, aluminum adatoms are imaged as protrusions with a large corrugation [1]. Images with a positive tip bias always had less corrugation, in agreement with other STM experiments [1]. As can be seen in this image, a well-ordered $(\sqrt{3} \times \sqrt{3})R30^\circ$ structure can be observed on the upper and lower terrace, although there is clearly some local disorder at the step edge. This might be due to the rapid quenching process that did not allow the step edge to build kinks fully quantized by $(\sqrt{3} \times \sqrt{3})R30^\circ$ unit cells. A similar

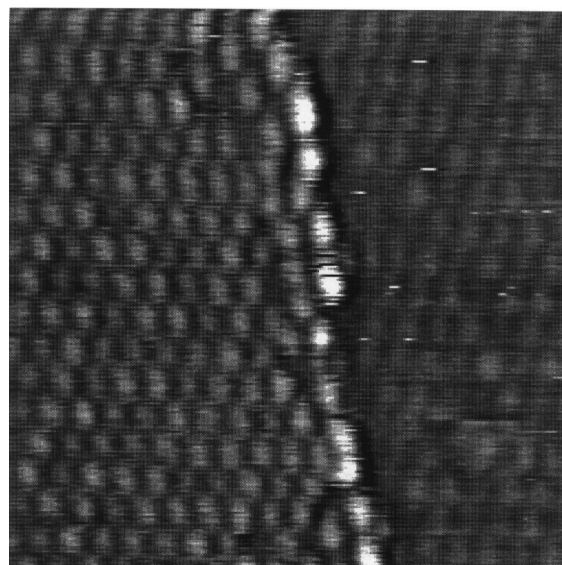


Fig. 3. Empty-state STM image of the same sample as in Fig. 2. The scan size is $135 \times 135 \text{ \AA}^2$, the tip bias is -2 V , and the tunneling current is 1 nA . The $[\bar{2}11]$ direction is oriented from left to right in this image.

observation has been made on clean Si(111) surfaces: slowly cooled, well-equilibrated samples only show kinks with a size equal to the unit cell of the (7×7) reconstruction, whereas kinks on quenched samples do not have this constraint [18]. We thus estimate that the equilibration temperature for the structure is very close to the disordering temperature of 765°C .

To quantify the surface morphology shown in Fig. 2, we analyzed the amount of meandering of single-layer-height steps and the terrace width distribution from a few images taken at different places on the sample. Fig. 4 shows the correlation function $F(y) = \langle [x(y) - x(0)]^2 \rangle$ as a function of the step-edge distance, y , separating two points $x(y)$ and $x(0)$ on the step edge. Note that x is the coordinate perpendicular, and y is the coordinate parallel to the step edge. As expected from continuum theory predictions, $F(y)$ increases linearly for small separations y [19]. It is remarkable that $F(y)$ is linear over a range that is more than twice as large as the average step-step separation, which is 135 \AA . However, as can be seen in Fig. 4, the mean square displacement $F(y)$ of the step position in the linear regime is still small compared to the

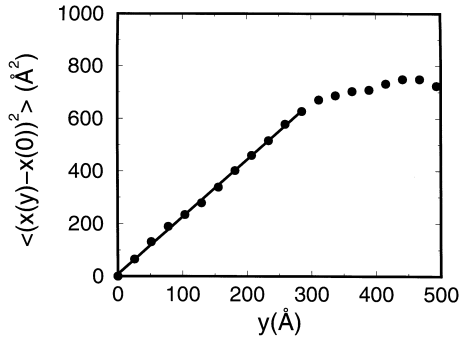


Fig. 4. Step correlation function $F(y) = \langle [x(y) - x(0)]^2 \rangle$ averaged over 30 steps and a total step length of about $3 \mu\text{m}$. The straight line is a fit to the data for small values of y .

square of the average step–step separation. For larger step–edge distances, the slope decreases because of the repulsive interaction between steps. From the initial slope of $F(y)$ for a small value of y , one can estimate the diffusivity $b^2(T)$ of a step given by:

$$F(y) = \frac{b^2(T)}{a_{\parallel}} y, \quad (1)$$

where a_{\parallel} is the lattice constant parallel to the step edge. From the slope of the straight line in Fig. 4, $b^2(T)/a_{\parallel} = 2.2 \text{ \AA}$. This value can be compared with the diffusivity of the clean Si(111)-(1 × 1) surface measured at a temperature of 900°C . As shown in Table 1, Alfonso et al. estimated a value of approximately 1 \AA from the analysis of snapshots of isolated steps [9,20]. Bartelt et al. determined a larger value of approximately 3 \AA from the analysis of equilibrium step fluctuations at the same temperature [21]. These values bracket that which we obtained for the Al-covered surface.

To obtain quantitative information about the step–step interactions, we also analyzed the terrace width distribution. We were careful to take data far away from the occasional small pinning centers, in regions where the steps were not curved. The final TWD was determined by measuring the terrace widths from three different images taken on different places on the sample, averaging over 60 steps in total. Note that two adjacent steps do not just give one data point, since the distance between two steps depends on the position parallel to the

step edge. To obtain the maximum available information, we first created an array of equidistant lines perpendicular to the average step–edge direction (i.e. along \hat{x}) in the STM images and then determined the terrace widths from the points of intersection between the step edges and lines. Fig. 5 shows the experimental distribution, $P(\ell)$, of terrace widths, ℓ , together with a fit to a Gaussian distribution: $P(\ell) = [1/w\sqrt{2\pi}] \exp[-(\ell - \langle \ell \rangle)^2 / 2w^2]$, with $w = 32 \pm 1 \text{ \AA}$, and $\langle \ell \rangle = 136 \pm 2 \text{ \AA}$. The quoted error bars are the standard deviation of the parameters determined from the fit.

From the Gaussian width, w , of the terrace width distribution, we can estimate the strength of the interaction between steps if we assume that it has a simple form. Even without an explicit energetic interaction between steps, the wandering of steps is limited by the rule that steps cannot cross. Consequently, there is an entropic repulsive interaction between steps, decaying as ℓ^{-2} with a magnitude proportional to $k_{\text{B}}Tb^2/a_{\parallel}$. In this case, the predicted ratio $w/\langle \ell \rangle$ is independent of temperature, with a value of about 0.42 [28]. The measured ratio is much less than this value: the observed Gaussian distribution is significantly narrower than the normalized distribution for steps with purely entropic repulsion [28]. It is, instead, characteristic of steps whose interaction is dominated by an energetic repulsion. If one assumes that this repulsive interaction has the form

$$U(\ell) = A\ell^{-n}, \quad (2)$$

a Gaussian distribution is an excellent approximation to the resulting equilibrium TWD [19], when the strength, A , of the repulsive interaction is sufficiently large. Specifically, for the physically important case of $n=2$, A must be much greater than $k_{\text{B}}Tb^2/4a_{\parallel}$ [20].

In this case, the width, w , of the Gaussian is given by [19]

$$w(T) = \left[\frac{k_{\text{B}}Tb^2(T)}{8n(n+1)Aa_{\parallel}} \right]^{1/4} \langle l \rangle^{(n+2)/4} \\ \rightarrow_{n=2} \left[\frac{k_{\text{B}}Tb^2(T)}{48Aa_{\parallel}} \right]^{1/4} \langle l \rangle, \quad (3)$$

where k_{B} is Boltzmann's constant.

Table 1

Measured values of the step diffusivity $b^2(T)/a_{\parallel}$ and the rescaled (dimensionless) Gaussian width of the terrace width distribution (TWD) $w/\langle\ell\rangle$ for different structures and adsorbate overlayers on Si(111) (These parameters have been used to estimate the step interaction strength, $A = (k_B T/48)(b^2/a_{\parallel})(w/\langle\ell\rangle)^{-4}$)

System	$T(^{\circ}\text{C})$	Diffusivity $b^2(T)/a_{\parallel}$ (\AA)	Width of TWD $w(T)/\langle\ell\rangle$	Step int'n A ($\text{eV}\cdot\text{\AA}$)	Cubic coefficient $g(T)$ ($\text{eV}\text{\AA}^{-2}$)	Reference
Si(111) (7×7) sngl hgt [$2\bar{1}\bar{1}$] steps	830	1 ± 0.2	0.26 ± 0.01	0.4 ± 0.1	0.036 ± 0.012 ($\tan\theta=0.05$) ^a	[20]
Si(111)-(7×7) sngl hgt [$\bar{2}11$] steps	830	<1.4	na	0.4 ± 0.1	<0.037	[20]
Si(111)-“ 1×1 ”	900	$0.8\text{--}2.9$	0.34 ± 0.02	$0.1\text{--}0.43$	$0.01\text{--}0.06$	[9,20,21]
Si(111) Br- 1×1	580	0.14 ± 0.03 ($\tan\theta=0.05$)	0.26 ± 0.01	0.06 ± 0.01	0.004 ± 0.001 ($\tan\theta=0.05$)	[22]
Si(113) $2^{\circ}\rightarrow[1\bar{1}0]$	875 950	8.3^b	0.066 ± 0.006	(9.3 ± 1.7) $\times 10^2$ ^b	(3.6 ± 0.7) $\times 10^2$ ^b	[23,24]
Si(111) Al ($\sqrt{3}\times\sqrt{3}$)R30 $^{\circ}$	770	2.2	0.24 ± 0.01	1.2 ± 0.2	0.1 ± 0.01	This paper
Si(111) Ga ($\sqrt{3}\times\sqrt{3}$)R30 $^{\circ}$	550	3.4	0.26	1.3 ± 0.6		[25]

The quoted error bars are one-sigma values. As reviewed elsewhere [20,26,27], the driving force for evolution of step-based morphologies is proportional to the coefficient $g(T)$ of the cubic term (in an expansion in terms of the tangent of the misorientation angle) of the projected (on to the terrace plane) surface free energy. Since, when the Gaussian approximation is valid, $g(T) = (\pi^2 k_B T/24 h^3)(b^2/a_{\parallel})[1 + \{1 + (1/12)(w/\langle\ell\rangle)^{-4}\}^{1/2}]^2$ is determined from the same two parameters, we include this important parameter here as well. [For estimation purposes, note: $g(T)\rightarrow_{A=0}(\pi^2 k_B T/6h^3)(b^2/a_{\parallel})$ and $g(T)\rightarrow_{w/\langle\ell\rangle < \pi^2 A/6h^3}$.]

^aThe measurement was done with steps misoriented by $\sim 3^{\circ}$ from the high-symmetry direction. In the limit $\theta\rightarrow 0$, the step-interaction free-energy parameter goes to 0.022 ± 0.005 eV \AA^{-2} .

^bCalculated using quoted [23,24] values of a_{\parallel} and a_{\perp} for room-temperature (3×2) rather than (1×1) values at the tabulated step “freezing” temperature. Note that for this misorientation direction, their convention for a_{\parallel} and a_{\perp} turns out to be the opposite of ours for general vicinal surfaces [19,20]. In Table 1, we use $T=T_b$, their “freezing” temperature of steps, $h=1.64$ \AA , and (in our notation) $a_{\parallel}=12.76$ \AA and $a_{\perp}=11.54$ \AA .

Physical predictions for step–step interactions induced either by an elastic strain field or by a direct dipole interaction all suggest a decay of the repulsive interaction proportional to ℓ^{-2} . Verification of the power-law decay of the step interaction and deduction of the decay exponent, n , requires a measurement of the width, w , of the distribution as a function of the average step separation $\langle\ell\rangle$. We have not made this measurement, but instead have made the very plausible assumption that the interaction between steps is dominated by a repulsive interaction given by Eq. (2) with $n=2$. This form of interaction is consistent with data for the clean Si(111) surface

measured with STM [10] and REM [9] over a large range of mean step separations $\langle\ell\rangle$. Using the $n=2$ form of Eq. (3) with the value determined for the diffusivity $b^2(T)$, we have $A=1.2\pm 0.2$ eV $\cdot\text{\AA}$ from the measured width of $P(\ell)$. The error bar on the value of A should be considered as the standard deviation.

Our primary interest regarding the repulsions is to see how the value of A for vicinal Si(111) surfaces with Al adsorbed compares to that for other Si(111) vicinal surfaces. Hence, we use the same expression as used in previous efforts [9,20,23,24]. The value of A deduced using Eq. (3) assumes that the repulsion is only between neigh-

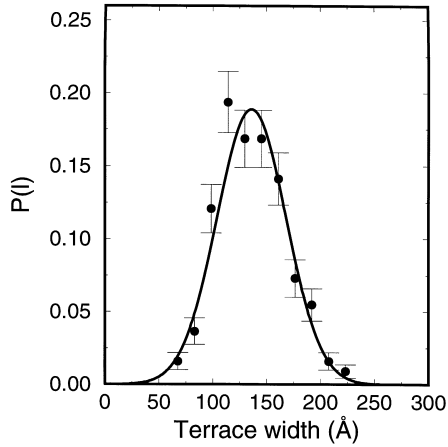


Fig. 5. Distribution of the terrace widths after deposition of a third of a monolayer of aluminum at 770°C and subsequent quenching to room temperature. Data are averaged over three images containing a total number of 60 steps. Error bars are calculated assuming the relative error to be \sqrt{N}/N , where N is the number of observations for a given terrace width. The solid line is a fit to a Gaussian distribution. Fit parameters are the width $w=32.3\pm 1.2$ Å and the average interstep distance $\langle \ell \rangle = 136\pm 2$ Å.

boring steps. For a uniform staircase of steps separated by $\langle \ell \rangle$ in which elastic interactions are not affected by intervening steps, A should be replaced by $1.08A$. (The simplest way [29] to include the effect of non-adjacent steps for a uniform staircase is to replace $A\ell^{-2}$ by $A\ell^{-2} \sum n^{-2} \equiv A\zeta(2)\ell^{-2} \simeq 1.64^+ A\ell^{-2}$, where ζ is the Riemann zeta function; this tactic greatly overestimates the effect of the other steps. Closer inspection of the derivation [19] shows that it is the curvature of the potential that matters. Thus, it is $Ax^2/6\ell^4$ that should be considered and replaced by $A\zeta(4)x^2/6\ell^4$, i.e. A is replaced by $\zeta(4)A = (\pi^4/90)A = 1.08\dots A$. Thus, neglecting multistep interactions (if they are present) leads to an overestimation of A by at most about 8%.)

There have also been recent suggestions that the value of A in Eq. (3) is overestimated by a more considerable factor, about 3, according to Barbier et al. [30–32] and Ihle et al. [33]. They claim that the Gruber–Mullins Gaussian approximation [19] underestimates the mean-square width of the TWD of energetically repelling steps by nearly a factor

of 3 (for a given value of A), or equivalently the width of the Gaussian by a factor slightly less than 2. However, we find [34] that – on the basis of comparisons with exact results and analytical approximants – Eq. (3) is a fine approximation for variance about 0.1, so $w/\langle \ell \rangle \approx 0.3$. It is very unlikely to deteriorate drastically for 0.26 (even if it turns out to do so for much narrower widths). Even if there were a multiplicative error – which is evidently not the case in general – we note again that it is the relative sizes of A for the various systems that are of greatest interest.

Our key finding is that, unlike the diffusivity, the repulsive interaction between steps determined from the terrace width distribution is distinctly different from values for the clean surface, as shown in Table 1. For the $\text{Al}-(\sqrt{3} \times \sqrt{3})\text{R}30^\circ$ structure, the estimated step interaction strength is three to 10 times as large as that measured for the clean $\text{Si}(111)-(1 \times 1)$ surface ($A=0.15$ eV-Å) [9,20], and about three times as large as the value measured for the (7×7) surface ($A=0.4$ eV-Å) [20].

4. Discussion

Our statistical analysis of STM images clearly shows that a change in the equilibrium crystal surface occurs during Al deposition at temperatures above the order–disorder phase transition of the $(\sqrt{3} \times \sqrt{3})\text{R}30^\circ$ structure. Whereas the clean vicinal $\text{Si}(111)$ surface is unstable with respect to facetting into (111) oriented facets with intervening high-density step bunches, an array of approximately equally spaced single-layer steps has been found for the aluminum-covered surface. As shown by our STM data, thermal equilibration to this new structure is kinetically hindered at the normal preparation temperature of 650°C for the $(\sqrt{3} \times \sqrt{3})\text{R}30^\circ$ structure. At this temperature, the morphology of the clean surface remains mostly unchanged, e.g. steps are still concentrated in bunches that separate large terraces. This observation suggests that the mobility of steps is low at this temperature, well below the temperature at which the $(\sqrt{3} \times \sqrt{3})$ reconstruction occurs. A similar phenomenon can be observed for the clean

surface, where steps are essentially immobile if the very stable (7×7) reconstruction is formed on the surface. However, above the disordering temperature for the (7×7) reconstruction, steps are highly mobile in the Si(111)-(1×1) phase, and equilibrium step fluctuations of the order of 100 \AA s^{-1} are measurable with REM [21].

From our quantitative analysis of STM images, we determined the diffusivity of steps and the strength of the repulsive step–step interaction. The results of our analysis are shown in Table 1, with a comparison to the values for other structures observed on Si(111). The diffusivity is in the same range as the values reported in the literature for the clean Si(111)-(1×1) surface [9,20,21]. However, the repulsive interaction between steps is strongly enhanced (by a factor of three to 10) by the aluminum adsorption. To understand this finding, we consider the physical origin of the repulsion.

If the step repulsions are due to elastic effects [35] – a common and physically reasonable assumption – then the interaction strength A can be related to the surface stress, σ , through the well-known equation [36,37]

$$A = \frac{2}{\pi E_2} (\sigma^2 h^2 + p_x^2), \quad (4)$$

where h is the step height, p_x is the in-plane dipole moment, and $E_2 \equiv E/(1-\nu^2)$ is the two-dimensional analogue of Young's modulus, E , with ν being Poisson's ratio. Since p_x is unknown, it is often just tacitly neglected (e.g. by replacing the parenthetical factor in Eq. (4) by τ^2 and calculating this torque about \hat{y} from just $\tau = \sigma h$). This approximation is generally adequate for metal surfaces, but Stewart et al. [38] have cast some doubt on its suitability for Si(111)-(7×7). They measure the tangential dipole moment p_x to be $1.46 \pm 0.3 \text{ eV \AA}^{-1}$, nearly thrice their computed normal dipole moment σh of $0.58 \pm 0.04 \text{ eV \AA}^{-1}$. In their work, the value of A then appears to be dominated by p_x . However, Wei et al. [39] can account well for the distribution of single and triple height steps on vicinal Si(111)-(7×7) by assuming $A \propto (\sigma h)^2$, which suggests that the stress term is dominant. Also, as tabulated and discussed

elsewhere [20,26,40], there is a surprisingly good (factor of two) agreement between the measured strength of the step interactions for single-height steps on clean vicinal Si(111) surfaces and values of A obtained using Eq. (4) with theoretical estimates of the surface stress and the in-plane dipole term set to zero. (The values of A , estimated from surface stress, in table 2.5 of Ref. [40] are about half the corresponding values in table 5 of Ref. [20] or Ref. [26] deduced from measured widths of TWDs using Eq. (3). Note that the high-temperature disordered phase is compared with calculations [41] for the (2×2) phase, whereas the (7×7) is compared with calculations for the (1×1) [42] plus the measured difference between that and the (7×7 .) This good agreement was obtained for both the low-temperature [(7×7)] structure and the high-temperature (“disordered”) structure. In the following, we will compare the expected values of the step interaction strength, A , based on the stress-term only in Eq. (4) with our measured values. We will then discuss the discrepancies in terms of the omission of the in-plane dipole term and other uncertainties in the application of Eq. (4).

An important assumption in the derivation of Eq. (4) is isotropy of the surface. Fortunately, this approximation is adequate for Si(111). (The anisotropy factor $(2c_{44} + c_{12} - c_{11})/c_{11}$ is 0.34 for Si [38].) To obtain values for the elastic modulus E_2 , Stewart et al. [38] performed a Voigt average over the stiffness tensor; alternatively, values for a particular surface orientation can be taken [43]. In Ref. [38], the value $E_2 = 1.08 \text{ eV \AA}^{-3}$ was used. Taking values for E_{111} and ν_{111} of Si from Ref. [43] – in which it was indicated that, conveniently, these moduli are invariant in the (111) plane – we find $E_2 = 1.132 \text{ eV \AA}^{-3}$. It is not clear which method is preferable, but in the present case, the difference is a mere 5%. We use $E_2 = 1.132 \text{ eV \AA}^{-3}$.

Only a limited amount of reliable information – computed or measured – is available about the surface stresses of specific systems. In particular, we found no values reported for the surface stress of $(\sqrt{3} \times \sqrt{3})\text{R}30^\circ \text{ Al}$ on Si(111). However, the stress of $(\sqrt{3} \times \sqrt{3})\text{R}30^\circ \text{ Ga}$ on this substrate –

which has the same T_4 adsorption site and similar local geometry (though a different-symmetry bonding orbital) [44] – has been found theoretically, using ab-initio pseudopotentials, to be 1.4 eV per (1×1) cell, somewhat less than the values of 1.66 for (2×2) Si(111) or 1.70 for $(\sqrt{3} \times \sqrt{3})R30^\circ$ Si(111) [41,45]. The values for the Si- (2×2) and Si- $(\sqrt{3} \times \sqrt{3})R30^\circ$ structures provide the best estimates of the stress of the high-temperature phase and are well below the ~ 2.5 eV per (1×1) cell estimated for the Si (7×7) structure [42,45]. It is reasonable to assume that the $(\sqrt{3} \times \sqrt{3})R30^\circ$ -Al has a stress value similar to the value of 1.4 eV for $(\sqrt{3} \times \sqrt{3})R30^\circ$ -Ga structure. Even if the true value were as much as 50% larger, it still would be smaller than the stress on the clean (7×7) Si(111) surface. Thus, if the step interactions were proportional to $(\sigma h)^2$ alone, our measured value of the step interaction would be unexpectedly large. This result could be due to a substantially larger tangential dipole p_x for the Al- $(\sqrt{3} \times \sqrt{3})R30^\circ$ phase than for the (7×7) Si(111) structure. Another possible source of uncertainty in calculating the value of A is that the theoretical calculations are for perfectly ordered structures at 0 K, whereas our structure was equilibrated near the disordering temperature of the $(\sqrt{3} \times \sqrt{3})R30^\circ$ structure, and thus represents a configuration with substantial thermal disorder. However, it is not obvious a priori whether disorder will increase or decrease surface stress.

Recently, an anomalously strong repulsive interaction between steps, leading to an extremely narrow terrace width distribution, was observed on vicinal Si(113) surfaces [23,24]. Because of the very narrow TWD, which occurs in spite of a large step diffusivity, the long-range repulsive step–step interaction has to be much stronger on vicinal Si(113) surfaces than that observed on vicinal Si(111) or Si(100) surfaces. The novel atomistic feature of Si(113) is the prevalence of rebonded atoms [46], with attendant puckering of the surface and many angles far from their ideal tetrahedral values [47]. As a result, it is not too surprising to find a dramatic increase in surface stress, as suggested by Table 1. However, in calculating A and even $b^2/a_{||}$ in Table 1, it is not clear what to use

for lattice parameters since, at room temperature, the steps apparently are quantized in terms of the (3×2) reconstruction, while even the (3×1) has gone at the “freezing” temperature of the Si(113) steps [48] that is presumed to mark the equilibration point of the observed distributions [23,24]. In any case, there is no evidence that anything similar to the complex rebonding of Si(113) occurs for intermediate-coverage Al on Si(111).

In summary, we have shown that aluminum adsorption can change the equilibrium morphology of faceted vicinal Si(111) surfaces dramatically. We have observed a complete debunching of steps if aluminum is deposited at temperatures above the order–disorder phase transition of the $(\sqrt{3} \times \sqrt{3})R30^\circ$ -Al/Si(111) structure. From a statistical analysis of STM images, we have been able to determine the diffusivity of steps and the repulsive step–step interaction after aluminum adsorption. While the measured diffusivity is in the same range as for the clean unreconstructed Si(111) surface, the repulsive interaction between steps is enhanced by a factor of three to 10, and the repulsive interaction between steps is about a factor of three larger than for the (7×7) reconstructed surface. Estimates of the step interactions from calculated values for the aluminum-induced surface stress are comparable to the values for the (1×1) structures and much less than the (7×7) , unlike the measured value, which is larger than both. A similar observation has recently been reported (see Table 1) for the $(\sqrt{3} \times \sqrt{3})R30^\circ$ -Ga/Si(111) surface [25]. This suggests that additional contributions to the step–step interactions, including the role of p_x , must be considered before a predictive understanding of step–step interactions can be accomplished.

Acknowledgements

This work has been supported by the NSF-MRSEC under grant DMR-96-32521 and the NSF-FAW under grant DMR-90-23453. One of us (C.S.) gratefully acknowledges a Feodor Lynen fellowship from the Alexander von Humboldt Foundation.

References

- [1] R.J. Hamers, Phys. Rev. B 40 (1989) 1657.
- [2] M. Yoshimura, K. Takaoka, T. Yao, T. Sato, T. Sueyoshi, M. Iwatsuki, Mater. Res. Soc. Symp. Proc. 295 (1993) 157.
- [3] K. Takaoka, M. Yoshimura, T. Yao, T. Sato, T. Sueyoshi, M. Iwatsuki, Phys. Rev. B 48 (1993) 5657.
- [4] T. Michely, M.C. Reuter, R.M. Tromp, Phys. Rev. B 53 (1996) 4105.
- [5] R.J. Phaneuf, E.D. Williams, Phys. Rev. Lett. 58 (1987) 2563.
- [6] R.J. Phaneuf, E.D. Williams, N.C. Bartelt, Phys. Rev. B 38 (1988) 1984.
- [7] R.J. Phaneuf, N.C. Bartelt, E.D. Williams, W. Swiech, E. Bauer, Phys. Rev. Lett. 67 (1991) 2986.
- [8] T.L. Einstein, in: W.N. Unertl (Ed.), Handbook of Surface Science, Vol. 1, North Holland, Amsterdam, 1996, p. 579.
- [9] C. Alfonso, J.M. Bermond, J.C. Heyraud, J.J. Métois, Surf. Sci. 262 (1992) 371.
- [10] X.S. Wang, J.L. Goldberg, N.C. Bartelt, T.L. Einstein, E.D. Williams, Phys. Rev. Lett. 65 (1990) 2430.
- [11] M. Giesen, Surf. Sci. 370 (1997) 55.
- [12] B.S. Swartzentruber, Phys. Rev. B 47 (1993) 13432.
- [13] J. Frohn, M. Giesen, M. Poensgen, J.F. Wolf, H. Ibach, Phys. Rev. Lett. 67 (1991) 3543.
- [14] Y.N. Yang, B.M. Trifas, R.L. Seifert, J.H. Weaver, Phys. Rev. B 44 (1991) 3218.
- [15] W.W. Pai, J.S. Ozcomert, N.C. Bartelt, T.L. Einstein, J.E. Reutt-Robey, Surf. Sci. 307–309 (1994) 747.
- [16] W.J. Wytenberg, R.M. Lambert, J. Vac. Sci. Technol. A 10 (1992) 3597.
- [17] R.Q. Hwang, E.D. Williams, R.L. Park, Surf. Sci. 193 (1988) L53.
- [18] J.L. Goldberg, X.-S. Wang, J. Wei, N.C. Bartelt, E.D. Williams, J. Vac. Sci. Technol. A 9 (1991) 1868.
- [19] N.C. Bartelt, T.L. Einstein, E.D. Williams, Surf. Sci. 240 (1990) L591.
- [20] E.D. Williams, R.J. Phaneuf, J. Wei, N.C. Bartelt, T.L. Einstein, Surf. Sci. 310 (1994) 451.
- [21] N.C. Bartelt, J.L. Goldberg, T.L. Einstein, E.D. Williams, J.C. Heyraud, J.J. Métois, Phys. Rev. B 48 (1993) 15453.
- [22] X.-S. Wang, E.D. Williams, Surf. Sci. 400 (1998) 220.
- [23] S. van Dijken, H.J.W. Zandvliet, B. Poelsema, Phys. Rev. B 55 (1997) 7864.
- [24] S. van Dijken, H.J.W. Zandvliet, B. Poelsema, Phys. Rev. B 56 (1997) 1638.
- [25] K. Fujita, Y. Kusumi, M. Ichikawa, Phys. Rev. B 58 (1998) 1126.
- [26] E.D. Williams, R.J. Phaneuf, J. Wei, N.C. Bartelt, T.L. Einstein, Surf. Sci. 294 (1993) 219.
- [27] E.D. Williams, Surf. Sci. 299–300 (1994) 502.
- [28] B. Joós, T.L. Einstein, N.C. Bartelt, Phys. Rev. B 43 (1991) 8153.
- [29] S. Kodiyalam, K.E. Khor, N.C. Bartelt, E.D. Williams, S. Das Sarma, Phys. Rev. B 51 (1995) 5200.
- [30] L. Barbier, L. Masson, J. Cousty, B. Salanon, Surf. Sci. 345 (1996) 197.
- [31] L. Masson, L. Barbier, J. Cousty, B. Salanon, Surf. Sci. 317 (1994) L1115.
- [32] L. Masson, L. Barbier, J. Cousty, B. Salanon, Surf. Sci. 324 (1995) L378.
- [33] T. Ihle, C. Misbah, O. Pierre-Louis, Phys. Rev. B 58 (1998) 2289.
- [34] T.L. Einstein, O. Pierre-Louis, preprint.
- [35] H. Ibach, Surf. Sci. Rep. 29 (1997) 193.
- [36] V.I. Marchenko, A.Ya. Parshin, Sov. Phys. JETP 52 (1980) 129.
- [37] J.M. Rickman, D.J. Srolovitz, Surf. Sci. 284 (1993) 211.
- [38] J. Stewart, O. Pohland, J.M. Gibson, Phys. Rev. B 49 (1994) 13848.
- [39] J. Wei, X.-S. Wang, J.L. Goldberg, N.C. Bartelt, E.D. Williams, Phys. Rev. Lett. 68 (1991) 3885.
- [40] E.D. Williams, N.C. Bartelt, in: W.N. Unertl (Ed.), Handbook of Surface Science, Vol. 1, North Holland, Amsterdam, 1996, p. 51.
- [41] R.D. Meade, D. Vanderbilt, Phys. Rev. Lett. 63 (1989) 1404.
- [42] R.E. Martinez, W.M. Augustyniak, J.A. Golovchenko, Phys. Rev. Lett. 64 (1990) 1035.
- [43] W.A. Brantley, J. Appl. Phys. 44 (1973) 534.
- [44] T. Hanada, H. Daimon, S. Nagano, S. Ino, S. Suga, Y. Murata, Phys. Rev. B 55 (1997) 16420.
- [45] R.D. Meade, D. Vanderbilt, in: M.A. Van Hove, K. Takayanagi, X.D. Xie (Eds.), The Structure of Surfaces III, Springer Series in Surface Science, Vol. 24, Springer, Berlin, 1996, p. 4.
- [46] J.H. Wilson, J.D. Todd, A.P. Sutton, J. Phys. Condens. Matter 2 (1991) 10259.
- [47] J. Wang, A.P. Horsfield, M.C. Payne, Phys. Rev. B 54 (1996) 13744.
- [48] H. Hibino, T. Ogino, Phys. Rev. B 56 (1997) 4092.